

# 2 Separation of nearby hadronic showers in the 3 CALICE SDHCAL prototype detector using 4 ArborPFA

---

R. Été<sup>a\*</sup>

<sup>a</sup> *Université de Lyon, Université Lyon 1, CNRS/IN2P3, IPNL, 4 Rue E. Fermi, 69622  
Villeurbanne Cedex, France*

5 *E-mail:* rete@ipnl.in2p3.fr

ABSTRACT: A new reconstruction algorithm, ArborPFA, is developed to separate nearby hadronic showers in the SDHCAL prototype. This intends to demonstrate the capability of high granularity hadronic calorimeters such as the SDHCAL to efficiently apply Particle Flow Algorithms. The reconstruction algorithm we present here uses the tree-like structure features of hadronic showers,  
6 that high granular calorimeters reveal, to associate hits belonging to each hadronic shower and to reduce confusions between two close-by showers. The results of these studies indicate a good single particle efficiency and reconstructed energy. A powerful separation down to distance of 5 cm was also pointed out.

---

\*Corresponding author.

## 8 **Contents**

9	<b>1. Introduction</b>	<b>2</b>
10	<b>2. The SDHCAL prototype</b>	<b>3</b>
11	<b>3. The Arbor particle flow algorithm</b>	<b>4</b>
12	<b>4. Single particle study</b>	<b>5</b>
13	4.1 Setup	5
14	4.2 Single particle analysis	5
15	<b>5. Separation of two close-by hadronic showers</b>	<b>8</b>
16	5.1 Overlay procedure and setup	8
17	5.2 Overlaid particles analysis	9
18	<b>6. Summary</b>	<b>13</b>
19	<b>A. ArborPFA algorithm</b>	<b>15</b>
20	<b>B. ArborPFA algorithm parameters</b>	<b>22</b>

22      Keywords: Particle flow; Calorimetry; ILC; SDHCAL

## 1. Introduction

To study the Higgs boson properties and to extend the discovery of new particles beyond the scope of LHC, linear (e.g ILC) and circular (e.g FCC or CEPC)  $e^+ e^-$  colliders are proposed. An important requirement of such a machine is to provide a good jet energy resolution ( $\Delta E/E \sim 3\text{-}4\%$ ) in order to distinguish between Z and  $W^\pm$  bosons as well as to study the Higgs boson properties.

The Particle Flow concept has been proposed to achieve the ILC benchmarks [2]. This algorithm aims to individually reconstruct particles using the most appropriate sub-detector for the energy and momentum measurement. An implementation of the particle flow algorithm called PandoraPFA has been developed [5] and successfully applied in ILD physics performance studies and to close-by hadronic showers separation

To apply efficiently the Particle Flow Algorithms, both good energy resolution and fine transverse and longitudinal segmentation should be provided by the *electromagnetic calorimeter* (ECAL) and the *hadronic calorimeter* (HCAL).

Different calorimeter technologies are currently under study by the CALICE collaboration to fulfill these requirements. In this framework, a *semi digital hadronic calorimeter* prototype (SD-HCAL) was built [1] and successfully tested at the CERN H6 test beam lines of the SPS (CERN) in 2012. With a transverse readout segmentation of  $1\text{ cm}^2$ , 48 sampling layers and good energy resolution [1], this calorimeter satisfies ILC requirements.

In this paper, we present an other approach of the particle flow : the ArborPFA approach. The algorithm has been designed for high granularity calorimeters and applied to SDHCAL test beam data. We propose to evaluate the performance of the algorithm on single pion events and to study the ability of the algorithm to separate two overlaid pion showers at different separation distances and energies.

## 2. The SDHCAL prototype

The SDHCAL prototype is a sampling calorimeter which consists of 48 layers alternating a 20 mm steel absorbers and a 6 mm gas resistive plate chamber (GRPC) with their embedded electronics. The gas gap between the two electrodes of the GRPC is 1.2 mm. 9216 pads (96 x 96) of 1cm<sup>2</sup> compose the readout of each chamber, leading to a total number of 442368 channels. Signals from particles crossing the gas gap are recorded on those pads in a 2-bits format corresponding to 3 thresholds on the induced charge. A complete description of the calorimeter setup and its features can be found in [1].

The test beam data used in this paper were taken at the CERN H6 beam line in 2012. The pion event selection is also performed according to the selection presented in [1].

The reconstructed energy of a single particle is computed as follows :

$$E_{rec} = \alpha(N_{hit}) \cdot N_1 + \beta(N_{hit}) \cdot N_2 + \gamma(N_{hit}) \cdot N_3 \quad (2.1)$$

where  $N_1$ ,  $N_2$  and  $N_3$  are the number hits of threshold 1, 2 and 3,  $N_{hit} = N_1 + N_2 + N_3$  and  $\alpha$ ,  $\beta$  and  $\gamma$  are quadratic functions of the number of hits  $N_{hit}$ . The nine parameters of these functions are extracted from a  $\chi^2$  minimization :

$$\chi^2 = \sum_{evt} \frac{(E_{beam} - E_{rec})^2}{E_{beam}} \quad (2.2)$$

This minimization was performed over all the hadronic events in the energy range [10, 80] GeV by step of 10 GeV. No weight is assigned event by event either per energy point. The linearity and energy resolution will be shown in section 4 dedicated to the single particle study.

### 3. The Arbor particle flow algorithm

The Arbor approach has been developed by the ALEPH collaboration and recently adapted [7] for ILD detector design. It is based on the idea that the hadronic shower development follows a tree-like topology.

Figure 1 shows an example of a shower development (left) where all main components of the shower are present : charged particles, neutral particles, electromagnetic and hadronic components. The same figure shows on the right a sampling calorimeter view of a shower interaction as seen in a highly granular calorimeter. The black arrows drawn on this view suggest the tree-like topology development of the shower.

With such an approach, the shower reconstruction follows a principle close to the underlying physics.

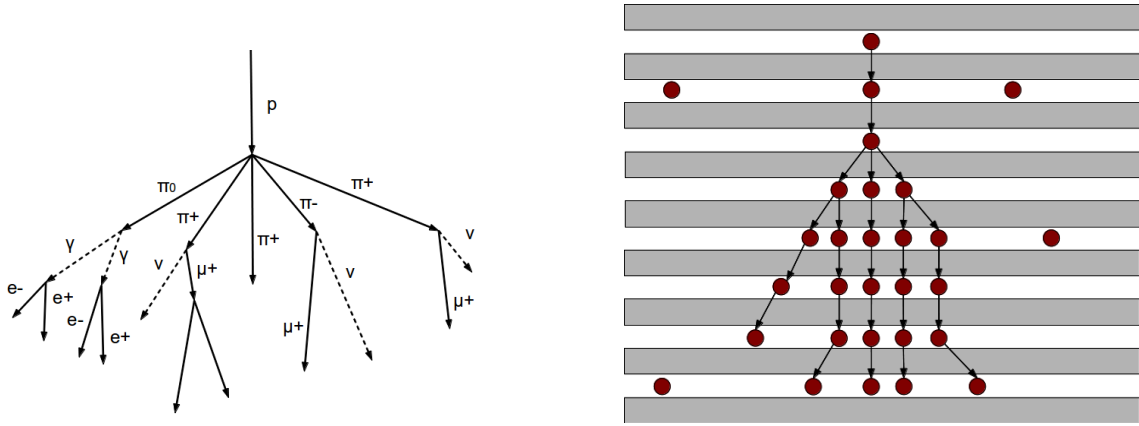


Figure 1: Left : schematic view of an induced proton shower. Right : schematic view of a reconstructed shower in a calorimeter with calorimeter hits (red)

The algorithm we used here is implemented using the PandoraSDK API as a toolkit for generic PFA development [6]. The API is used in a Marlin [4] C++ processor as part of the reconstruction chain in ILCSoft [8]. A complete description of the algorithm can be found in Appendix A

## 4. Single particle study

### 4.1 Setup

To study the single particle performance of the algorithm, we use the SDHCAL charged pion data taken at CERN on the H6 line of SPS in 2012 from 10 GeV up to 80 GeV. In order to select only pions, an event selection is performed as described in [1].

To correctly emulate a charged pion for the reconstruction program and since there was no tracker in front of the SDHCAL during beam tests, a fake track is created in front of the calorimeter. A global barycentre of all hit positions in the transverse plane (X and Y axes) is calculated. A new barycentre is then calculated using only hits in the 4 first layers and within a region of 8x8 cells around the global barycentre in the X and Y directions. This defines the shower entering point in the first layer. From the entering point of the shower, a straight track is created along the beam axis (Z direction) with momentum equal to that of beams.

The calorimeter hits and the created track are then loaded into the PandoraSDK toolkit [6] within a single hcal endcap geometry (no magnetic field) with the SDHCAL prototype dimensions and processed by the ArborPFA algorithms. An event display of a single pion event is shown on figure 2.

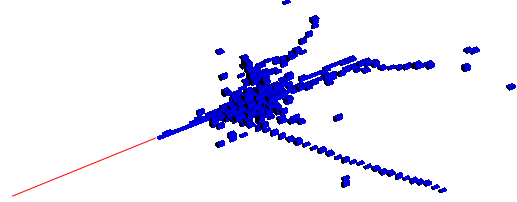


Figure 2: Event display of a 50 GeV pion shower in the SDHCAL detector

### 4.2 Single particle analysis

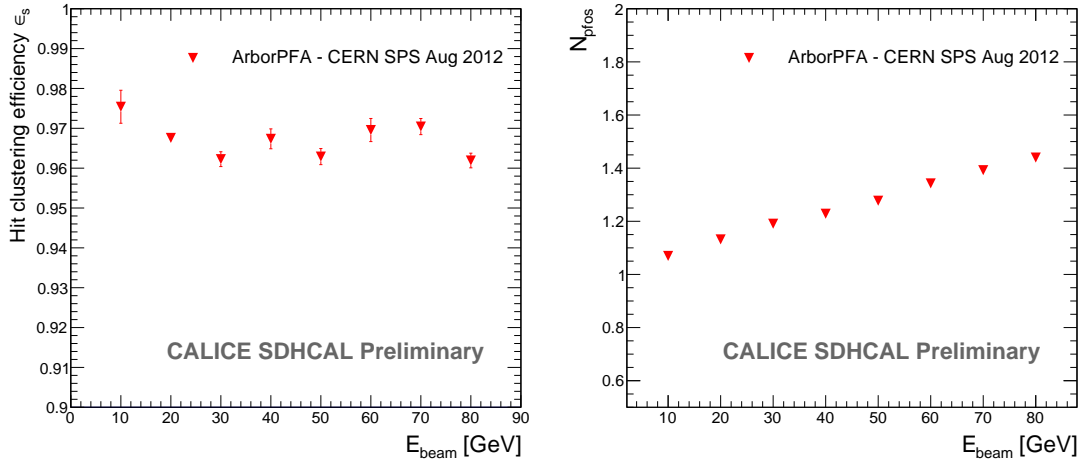


Figure 3: Hit clustering efficiency (left) and the mean number of reconstructed particles (right) after ArborPFA reconstruction on single pion shower events with the SDHCAL prototype

101 We define the efficiency of the single particle reconstruction, or the hit clustering efficiency  
 102  $\epsilon_s$  as the fraction of hits recovered by the ArborPFA program and correctly attached to track in  
 103 front of the calorimeter. Figure 3 shows the mean efficiency of the single particle reconstruction  
 104 (left) and the mean number of reconstructed particles (right) as a function of the beam energy after  
 105 applying ArborPFA. It shows a constant efficiency of over 96% over the whole beam energy range.  
 106 Since the number of hits increases with the energy, the number of missed hits in the reconstructed  
 107 charged particle also increases. Consequently, the mean number of reconstructed particles shows an  
 108 increase which is directly due to shower splitting. This number grows up to 1.45 particles at 80 GeV  
 109 but has only a small impact on the reconstructed energy and energy resolution because the small  
 110 additional clusters represent a small amount of energy. Indeed, figure 4 shows the reconstructed  
 111 energy and energy resolution of a single charged pion before and after running the ArborPFA  
 112 program.

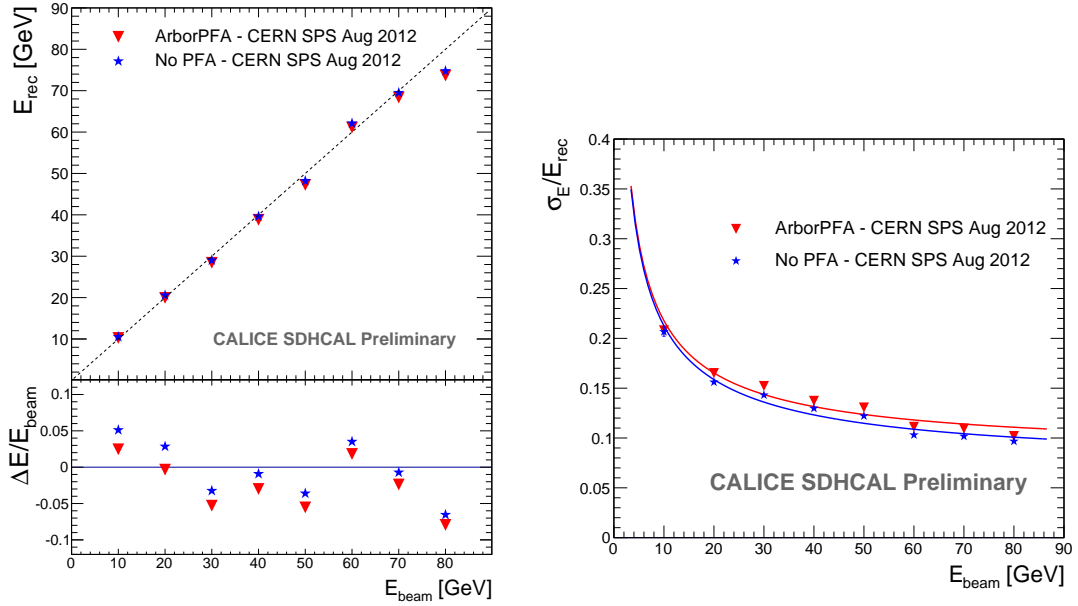


Figure 4: Reconstructed energy (left) and energy resolution (right) before (blue) and after (red) ArborPFA reconstruction on single pion shower event with the SDHCAL prototype

113 The deviation from linearity is shown below the reconstructed energy and is defined as :

$$\Delta E/E_{beam} = (E_{rec} - E_{beam})/E_{beam} \quad (4.1)$$

114 These energy points are extracted using two fits of the energy distributions : i) a gaussian  
 115 distribution fit over the full reconstructed distribution is first performed. The mean  $\mu_{E,first}$  and  
 116 width  $\sigma_{E,first}$  are extracted, and ii) a second gaussian fit is then performed over the range  $[\mu_{E,first} - 1.5 \cdot \sigma_{E,first} ; \mu_{E,first} + 1.5 \cdot \sigma_{E,first}]$ . From the latter, we extract the final values of the reconstructed  
 117 energy and energy resolution defined as the mean  $\mu_E$  and the width  $\sigma_E$  respectively of the gaussian  
 118 fit (same procedure applied in [1]). The efficiency plot has shown that some hits are missing  
 119 after reconstruction so it is expected to have a small energy decrease in the reconstructed energy.  
 120

121 Nevertheless, the linearity is still within 8% as before applying the reconstruction. The energy  
122 resolution is also not so much affected after reconstruction.



## 5. Separation of two close-by hadronic showers

The ability of a particle flow algorithm to disentangle close-by showers is a key point for the reconstruction in detectors such as ILD of the ILC. To study the confusion between neutral and charged hadrons and the ability of the ArborPFA algorithm to disentangle them, we again use the same test beam data of the SDHCAL prototype. Two different pion showers are first overlaid in the same event and the ArborPFA algorithm is run on the overlaid event with the same parameters as for the single particle study. An analysis of the separation is then performed in order to extract the performance of the algorithm.

### 5.1 Overlay procedure and setup

In order to study the separation of nearby hadronic showers, two events from test beam data are overlaid in one event. We have chosen to overlay 10 GeV pion events and pion events at different energies from 10 GeV to 50 GeV, in steps of 10 GeV. The distance between shower entry points was scanned between 5 cm and 30 cm in steps of 5 cm. The choice of this energy range is motivated by the fact that it is the typical single particle energies foreseen at the ILC within jets [3].

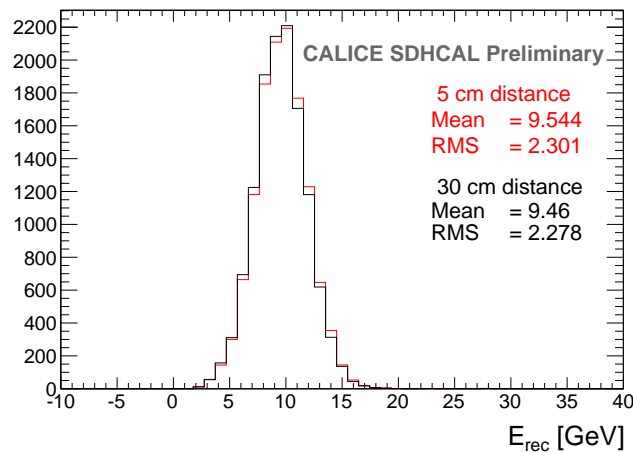


Figure 5: The reconstructed energy of the 10 GeV neutral hadron after the overlay procedure with a 50 GeV charged hadron with a separation distance of 30 cm (black) and 5 cm (red)

The overlay event algorithm is processed as follow :

1. The entering track segments of the two showers are determined as for the single particle case. This allows to identify the shower entering points and starting points.
2. The hits belonging to the 10 GeV pion primary track segment are removed from the event in order to emulate a neutral hadron shower.
3. The two showers are then centred along the X and Y axis at the center of the calorimeter. No shift is performed on the Z direction (beam line).

- 144 4. The showers are then shifted along the X axis by a distance of  $-d/2$  for the neutral hadron and  
145  $+d/2$  for the charged particle, where  $d$  is the distance to the calorimeter center in cm.
- 146 5. The two events are then overlaid. At this step a problem may occur : while mixing the  
147 showers in the event, pair of hits may overlap in the same cell. Knowing that we are using a  
148 semi digital readout and that the information of the deposit charge in each cell is not available  
149 in the data, we need to assign a new threshold by using an approximation. The most intuitive  
150 one is to keep the highest threshold of the two hits. Figure 5 shows the reconstructed energy  
151 of the 10 GeV neutral hadron overlaid with a 50 GeV charged hadron at 30 cm distance (left)  
152 and 5 cm distance (right). The latter case is the worst one that can appears in this study given  
153 the energy points and the distances we have chosen. By comparing the two plots, we can see  
154 that the effect of this approximation on the reconstructed energy is negligible.
- 155 6. The hits are tagged with respect to our initial showers. The overlaid hits are tagged differently  
156 so that the information on the overlaid hits can be retrieved after reconstruction.
- 157 7. A new event is created containing the overlaid showers and the entering point of the charged  
158 particle track after shifting. An example is shown on figure 6.

159 Figure 6 also shows a small energy deviation of -0.54 GeV for the 30 cm case. With respect  
160 to the reconstructed energy after running ArborPFA shown on figure 4 (left), a drop of -0.8 GeV is  
161 observed and is due to the track segment hits removal while overlaying the two showers.

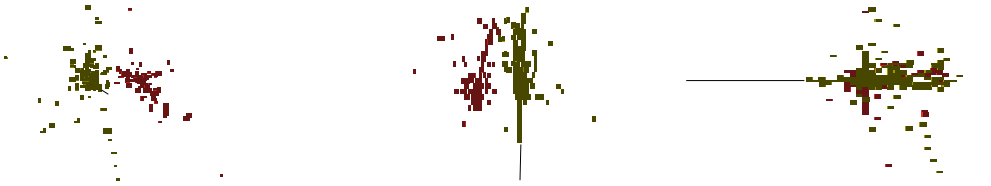


Figure 6: Display of a 10 GeV fake neutral hadron overlaid with a 30 GeV charged hadron separated by 20 cm in three different views (XoY on left, XoZ in center and YoZ on right). Colours correspond to the reconstructed PFOs after running the ArborPFA program. The black straight line is the fake track generated in front of the calorimeter.

## 162 5.2 Overlaid particles analysis

163 Figure 7 shows the mean number of PFOs after running the ArborPFA program on a 10 GeV  
164 fake neutral hadron overlaid with a charged hadron at different energies and different separation  
165 distances. The behaviour at a large separation distances where the number of PFOs increases with  
166 the charged particle energy matches the behaviour of the number of PFOs in the single particle  
167 study. We can also see that the sum of the number of PFOs for the single particle is compatible  
168 with the number of PFOs for the overlay. The mean number of PFOs is stable at large separation  
169 distances but slightly decreases at 5 cm from about 2.1 PFOs down to about 1.8 PFOs due to the  
170 showers overlaps and resulting confusions.

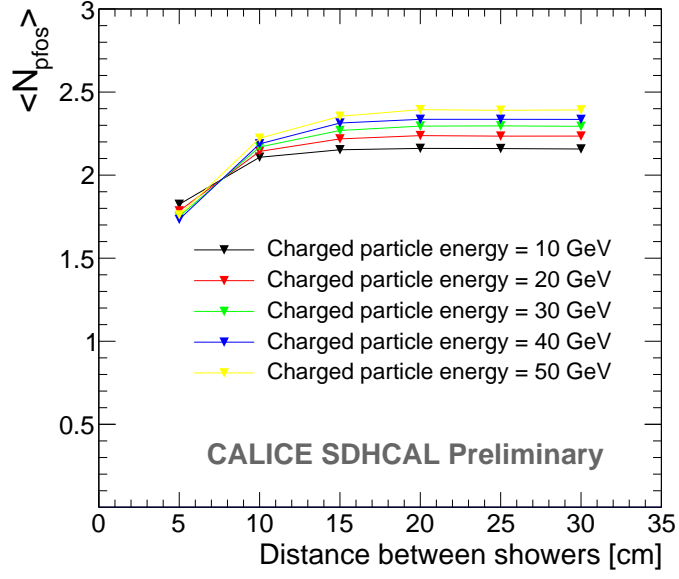


Figure 7: The mean number of PFOs after running the ArborPFA program on overlaid particles.

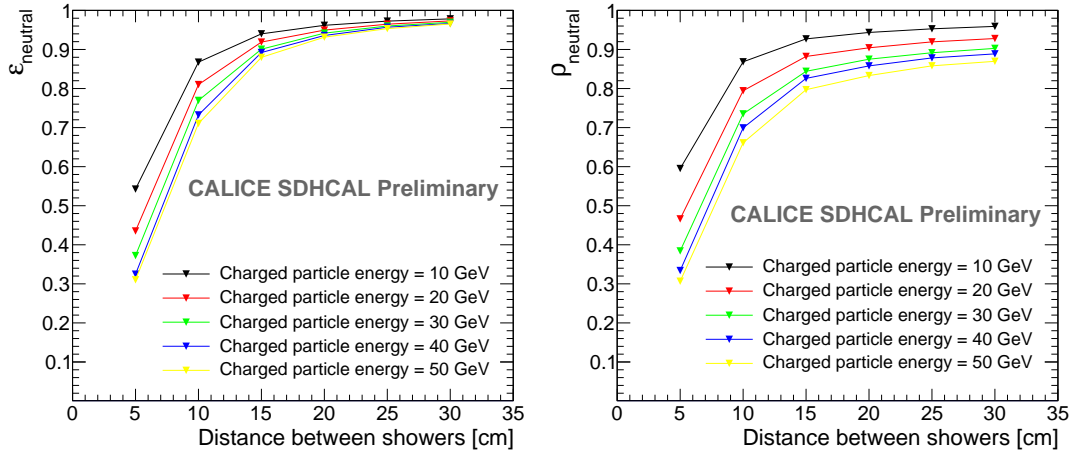


Figure 8: The efficiency (left) and purity (right) of the 10 GeV neutral hadron after reconstruction

171 To quantify the separation, we define the efficiency and the purity related to the reconstruction  
 172 of one of the two related showers as :

$$\varepsilon = \frac{N_{hit_{good}}}{N_{hit_{ini,tot}}} \quad (5.1)$$

$$\rho = \frac{N_{hit_{good}}}{N_{hit_{rec,tot}}} \quad (5.2)$$

174 with  $N_{hit_{good}}$  the number of hits that initially belong to the particle and correctly assigned

175 after reconstruction,  $N_{hit_{rec,tot}}$  the total number of hits of the reconstructed shower and  $N_{hit_{ini,tot}}$   
 176 the total number of hits of the particle before reconstruction.

177 Figure 8 shows the efficiency (left) and the purity (right) of the neutral hadron for different  
 178 charged particle energies and different separation distances. In the same way as for the mean  
 179 number of PFOs, at small distances the two showers start to overlap and confusions appear in  
 180 the reconstruction. Thus, some hits of the neutral hadron are assigned to the charged one (and  
 181 vice versa) and the efficiency and purity decrease. At large separation distances, the purity does  
 182 not tend to 100%. This is due to the last performed algorithm (small neutral fragment algorithm)  
 183 which merges small neutral cluster fragments to their closest parent cluster, without considering  
 184 the parent cluster size or energy. Since the number of neutral fragments for a single hadron particle  
 185 increases with the energy, a non-negligible part of the charged hits is assigned to the neutral hadron,  
 186 leading to a decrease of its purity.

187 Figure 9 (left) shows the fraction of events in which at least one neutral hadron has been recon-  
 188 structed. As expected, the number of reconstructed neutral particles decreases with the separation  
 189 distance. From 30 cm down to 15 cm, this fraction is stable and greater than 97%. At 10 cm,  
 190 confusions becomes significant and the neutral hadron is sometimes merged with the charged one,  
 191 leading to a small decrease of this fraction. At 5 cm, we can see that the fraction strongly depends  
 192 on the charged particle energy and goes from 73% of reconstructed events for the 10 GeV charged  
 193 particle case down to 60% at 50 GeV.

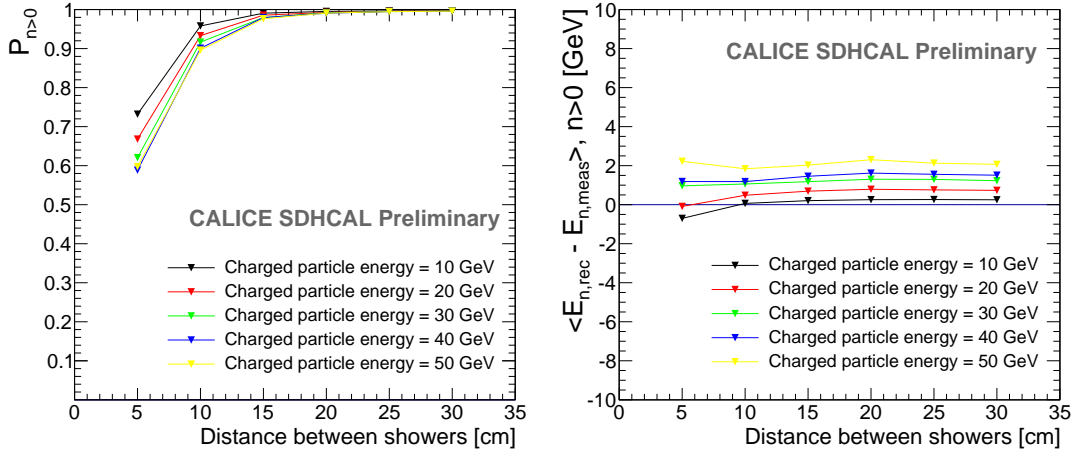


Figure 9: Left : The fraction of events where at least one neutral hadron has been reconstructed.  
 Right : The mean difference between the reconstructed energy and the measured energy before  
 reconstruction for which at least one neutral hadron has been reconstructed.

194 We define the reconstructed neutral energy as the sum of the neutral particle energies and the  
 195 measured neutral energy as the estimated energy before reconstruction. Figure 9 (on the right)  
 196 shows the mean difference between the reconstructed neutral energy and the measured neutral en-  
 197 ergy when at least one neutral hadron has been reconstructed. In the same way as for the purity, the  
 198 mean reconstructed neutral energy increases with the charged particle energy. This plot also shows  
 199 a flat behavior of the reconstructed neutral energy with the separation distance. This means that

200 the reconstruction of the neutral hadron at very small distance (5 cm) has a *binary-like* behaviour,  
201 either well reconstructed or completely merged with the charged hadron.

## 6. Summary

The ArborPFA, based on the tree-like structure of hadronic showers has been described in details.

A single particle study has been performed on SDHCAL test beam data taken at SPS at CERN during August and September 2012 [1]. Single pion showers have been selected and a track in front of the calorimeter has been created in order to emulate a track from a tracking detector.

The results show a good efficiency with more than 95% of hits assigned to the reconstructed charged particle over the energy range of 10 to 80 GeV. The mean number of PFOs shows a linear increase with the energy from 1.1 PFOs at 10 GeV to 1.4 PFOs at 80 GeV. Around 4% of hits are not clustered by the algorithm, leading to a small decrease in the clustered energy response and a small degradation of the energy resolution with respect to the case in which all hits are considered.

The ability of the algorithm to separate nearby hadronic showers was also investigated. Two different charged hadron showers with different energies from the same test beam data set have been overlaid in the same event with different separation distances. For the 10 GeV pion shower, the track segment inside the calorimeter has been identified and removed from the event in order to emulate a neutral hadron particle. For the other particle, a track has been generated in front of the calorimeter and pointing on the particle entry point, as for the single particle case.

The results showed a neutral hadron recovery higher than 90% until 10 cm separation distance where a non negligible confusion starts to appear.

The difference between the reconstructed energy and the measured energy of the neutral hadron in the case where at least one neutral hadron has been reconstructed showed an increase with the charged hadron energy for all the separation distances due to the small neutral fragment merging algorithm. At small separation distance (5cm), the difference stays constant and shows that the neutral hadron reconstruction has a *binary-like* behaviour, either a very good reconstruction or merged in the charged hadron.

This work will be extended shortly to include the electromagnetic calorimeter as well as the other sub-detectors in the framework of the ILD detector with the aim to separate charged and neutral hadrons produced in jets to improve on the PFA performances.

## 229 References

- 230 [1] Calice Collaboration, *First results of the CALICE SDHCAL technological prototype*, CAN-037
- 231 [2] J. Carwardine *et al.*, *International Linear Collider Technical Design Report*. 1) Executive Summary, 2)
- 232 Physics, 3) Accelerator, 4) Detectors. 12 June 2013
- 233 [3] O. Lobban, A. Sriharan, R. Wigmans, *On the energy measurement of hadron jets*, *Nucl. Instrum. Meth.*
- 234 **A495** (2002) 107-120
- 235 [4] F. Gaede, Marlin and LCCD: Software tools for the ILC, *Nucl. Instrum. Meth.* **A559** (2006) 177-180
- 236 [5] M. A. Thomson, *Particle Flow Calorimetry and the PandoraPFA Algorithm*,
- 237 `phys.int-det/0907.3577`
- 238 [6] J. S. Marshall, M. A. Thomson, *The Pandora Software Development Kit for Pattern Recognition*,
- 239 `phys.int-det/1506.05348`
- 240 [7] M. Ruan, *Arbor, a new approach of the Particle Flow Algorithm*, Proceeding of CHEF 2013.
- 241 `hep-ex/1403.4784`
- 242 [8] ILCsoft, 2012. <http://ilcsoft.desy.de/portal>
- 243 [9] ROOT, 1995-2015, <https://root.cern.ch/drupal>

## 244 A. ArborPFA algorithm

245 Before describing the algorithm in detail, a few definitions specific to ArborPFA need to be intro-  
246 duced :

247 **Object** An *object* is a calorimeter hit or a group of contiguous calorimeter hits within a layer  
248 that serves as a vertex for the ArborPFA algorithm. This was introduced for two reasons i) to  
249 provide a generalization of connections between *objects* without making any assumptions of what  
250 is contained in an *object*, ii) to overcome the pad multiplicity<sup>1</sup> inherent in the SDHCAL [1] and  
251 similar detectors.

252 **Flow direction** The flow direction is of two kinds : forward direction which is from upstream to  
253 downstream of the beam direction and backward direction for the opposite.

254 **Connector** A connector is a link between two *objects*. It has a weight and a direction.

255 **Connector depth** The connector depth is defined as the number of intermediary connectors link-  
256 ing two different objects.

257 **Tree** A tree is a set of *objects* connected in a tree topology, which means that for each object  
258 there is only one backward connector. An *object* without a backward connector is called a seed and  
259 an *object* without a forward connector is called a leaf.

260 **Cluster** A cluster is a set of trees.

261 **Particle flow object (PFO)** A particle flow object is a set of clusters and tracks<sup>2</sup>, which corre-  
262 sponds to a reconstructed particle.

263

264 Note that in the following algorithm descriptions, some parameters are labelled by a name or sym-  
265 bol, whose values are given in a separate Appendix B.

## 266 Pre-clustering phase

267 Before building trees, we need to create objects to  
268 connect with each other.

269 **Object creation** When a particle goes through the  
270 detector, several pads can be fired in a single layer,  
271 leading to a multiplicity greater than 1. To overcome  
272 this problem, intra-layer groups of hits are assembled  
273 using the nearest neighbour clustering algorithm (cor-  
274 ner neighbours not included). If a group contains more  
275 than 4 hits, it is split and each individual hit is consid-  
276 ered as a separate object. This generally happens in the  
277 shower core. If a group contains 4 or less hits, it is used

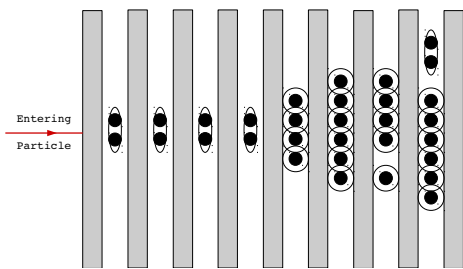


Figure 10: Schematic view of the object creation output. Small groups of contiguous calorimeter hits are grouped together (encircled).

<sup>1</sup>More than one pad could be fired when a particle crosses the gas gap.

<sup>2</sup>By *track* we mean one reconstructed by a tracking detector such as a TPC



278 to define a single object. This is the case for a mip or  
 279 more generally any isolated non-showering particle. Figure 10 shows the output of this algorithm  
 280 with encircled hits forming objects.

281 **Track segment<sup>3</sup> candidate tagging** In order to correctly reconstruct the primary track segment  
 282 in the calorimeter, track segment candidate *objects* are identified and tagged for future treatment.  
 283 For each object, we count the number of objects in the same layer within a distance of  $\Delta_{mip}$ . If this  
 284 number doesn't exceed  $N_{obj, cut}$ , the object is tagged as a track segment candidate object.

### 285 The main clustering phase - Connectors and trees

286 The main clustering algorithm consists of an iterative procedure using dedicated algorithms to  
 287 create and remove connectors (connector loop). At the end of this step, all objects are arranged in  
 288 a tree structure, which means that each object has at most one connector in the backward direction  
 289 and 0 or more in the forward direction.

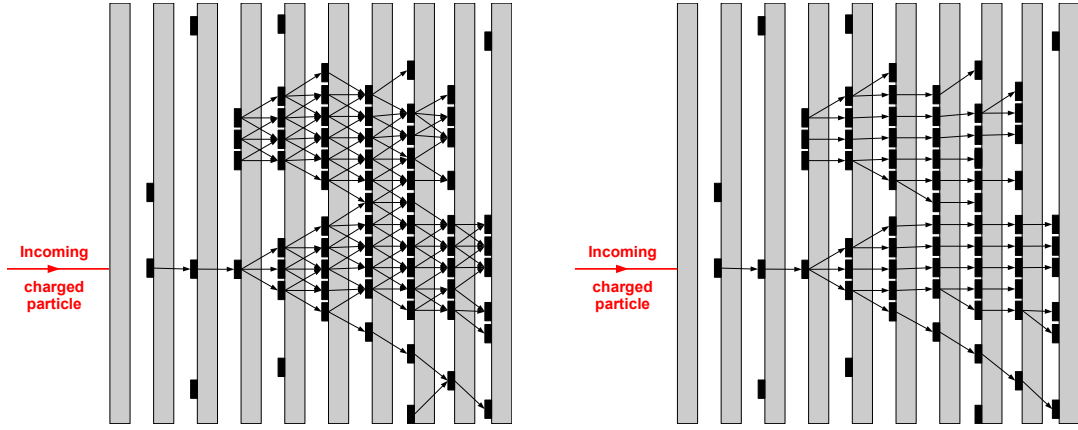


Figure 11: Schematic view of a neutral and a charged pion showers after the first connector seeding algorithm (left) and cleaning algorithm (right)

290 In the current implementation, the connector loop contains the following algorithms :

291 **Primary track connection** This algorithm aims to create connections between objects belonging  
 292 to the primary track segment of charged particles in the calorimeter. It consists mainly in creating  
 293 a sub-list of objects that are candidates for the primary track segments by using the objects tagged  
 294 as track segment candidates and the track extrapolations on the front of the calorimeter. Once this  
 295 list is built, the "*connector seeding 1*" algorithm and the "*connector cleaning 1*" algorithm are run  
 296 on only the sub-list objects.

297 **Connector seeding 1** We start by creating connections in the neighbourhood of each object. For  
 298 each object, we look for other objects in the  $N_{layers}$  next layers within a maximum distance  $\Delta_{max}$   
 299 and we create connections between them. As an example, Figure 11 (left) illustrates the output of  
 300 this algorithm.

---

<sup>3</sup>By *track segment* we mean a track produced by a charged particle in the calorimeter such as Minimum Ionizing Particles (MIP)

301 **Connector cleaning 1** Once connectors are created, we need to build a tree structure by keeping  
 302 only one connector in the backward direction for each object. We define the reference direction of  
 303 an object as :

$$\vec{C}_{ref} = w_{bck} \cdot \sum_{\sigma} \sum_b \vec{c}_{b,\sigma} - w_{fwd} \cdot \sum_{\delta} \sum_f \vec{c}_{f,\delta} \quad (\text{A.1})$$

304 where :

- 305 •  $w_{bck}$  ( $w_{fwd}$ ) is a global positive weight assigned to backward (forward) connectors
- 306 •  $\vec{c}_{b,\sigma}$  ( $\vec{c}_{f,\delta}$ ) is the direction of a backward (forward) connector at the connector depth  $\sigma$  ( $\delta$ )
- 307 from the considered object

308 The depth parameter  $\sigma$  has been fixed to 1 in all algorithms. The reference direction is a  
 309 vector that goes in the backward direction and indicates the most probable direction for a unique  
 310 backward connection. Then we need to assign which backward connector should be kept for the  
 311 tree building. Thus, for each backward connector of an object, we define the  $\kappa$  parameter as :

$$\kappa = \left( \frac{\theta}{\pi} \right)^{p_{\theta}} \cdot \left( \frac{\Delta}{\Delta_{max}} \right)^{p_{\Delta}} \quad (\text{A.2})$$

312 where :

- 313 •  $\theta$  is the angle between a backward connector and the reference direction of the considered  
 314 object,
- 315 •  $\Delta$  is the distance between the connected objects,
- 316 •  $p_{\theta}$  ( $p_{\Delta}$ ) is a power parameter for the normalized angle (distance)

317 The  $\kappa$  parameter quantifies the alignment with the reference direction within the range [0,1].  
 318 Smaller is this parameter, higher the alignment will be. The power parameters  $p_{\theta}$  and  $p_{\Delta}$  are to be  
 319 tuned depending on which variable we want to emphasize.

320 The chosen backward connector for the tree building is the one with the smallest  $\kappa$  parameter;  
 321 all others are removed from the list. The removal of connectors is done at the end of the algorithm  
 322 so that all connectors contribute to the evaluation of the reference direction.

323 **Connector seeding 2** This second step of connector seeding starts from the tree structure ob-  
 324 tained after the first connector cleaning algorithm. The goal of this second step is to create an  
 325 alignment of connectors within the shower. For each connector, more forward connectors are cre-  
 326 ated from the forward object of this connector by looking in a cone of half-angle  $\theta_c$  and a maximum  
 327 distance of  $\Delta_{max,c}$ . In the same way, additional backward connectors are created from the backward  
 328 object of this connector. A schematic view of this step is shown in figure 12.

329 **Connector cleaning 2** Here, we again need to clean up the backward connector list to end up  
 330 with only one connector per object. This last algorithm is similar to the first connector cleaning  
 331 except that the cleaning is done layer per layer starting from the downstream layers with a depth  
 332 parameter  $\delta$  strictly higher than one. For a given connector, this accentuates the alignment with the  
 333 forward ones. We end up then with a tree structure again.

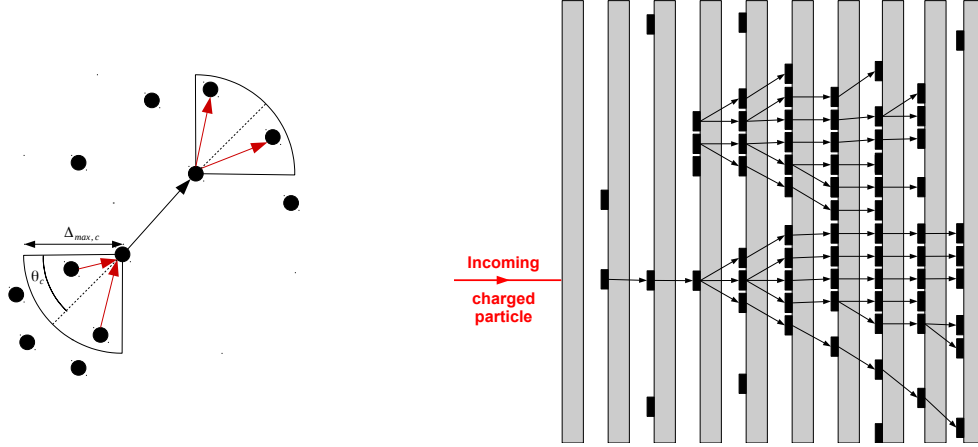


Figure 12: Left : Schematic view of the connector alignment procedure. In black, a considered connector and in red possible new connectors in backward and forward directions. Right : a neutral and a charged pion showers after the second connector cleaning algorithm

**Tree building** This step is straight-forward. Seed objects are identified and trees are built by recursively following the forward connected objects.

The following algorithms associate some of the trees with each other.

### Association algorithms

**Energy driven track cluster association** The track to cluster association is performed using three different pieces of information, the cluster energy, the track momentum and the cluster topology. We first look at the track projection on the calorimeter front face. Two different cases may occur :

- the particle has interacted before the calorimeter or in the first layer. In this case, many seed objects are found in the  $N_{layer}$  first layers at a maximum distance of  $\Delta_{track-cluster_1}$  of the track projection. Seed objects are then sorted by their distance to the track projection. The clusters associated to their seeds are then associated to the track progressively starting from the closest one until the difference between the track momentum and the total cluster energy is minimized. The clusters are then merged since they belong to the same cluster structure.
- the particle produced a track segment at least in the  $N_{layer}$  first layers and a seed object is found within a distance  $\Delta_{(track-cluster)_1}$  to the track projection. Since only a cluster starting with a track segment has to be associated, an additional distance cut  $\Delta_{(track-cluster)_2}$  between seed objects and the track projection is applied. This decreases the confusion for small separation distances between nearby particles. The same track-to-cluster association and cluster merging is then performed as above.

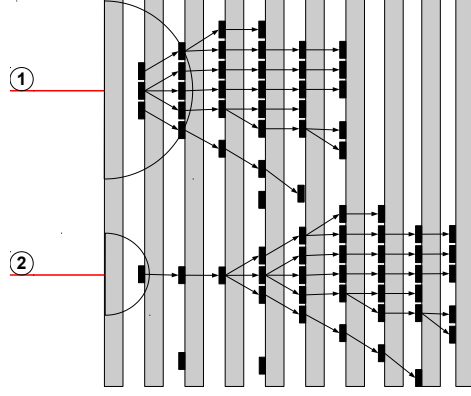


Figure 13: Schematic view of the energy driven track cluster algorithm.

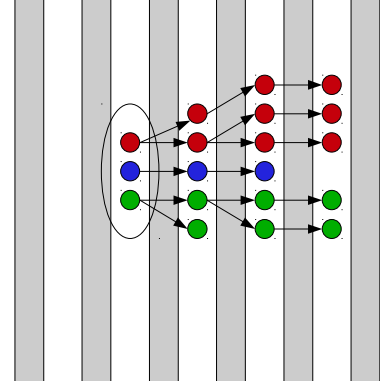


Figure 14: Schematic view of the neutral tree merging algorithm.

Figure 13 shows a schematic view of the two different scenarios. The upper one corresponds to the case where an early interaction is found, and the lower one where a primary track segment of a cluster is found.

**Neutral tree merging** This algorithm is designed for neutral particle interactions for which the first interacting layer contains a few seeds. Figure 14 shows a configuration in which three trees have been built (with three colours) for one neutral particle interaction. We can see that the seeds in the first interacting layer all belong to the same cluster. The trees having seeds closer than  $\Delta_{seed}$  and positioned in the same layer are merged.

**Pointing cluster association** This step aims at associating neutral fragments (daughter cluster) to other fragments which may be charged or neutral clusters (parent clusters). We start by identifying the clusters that have at least  $N_{objects}$  objects in at least  $N_{layer}$  contiguous layers. The selected cluster could be either a parent or a daughter cluster. Then we proceed as follows :

1. A linear 3D straight line fit is performed over the position of all the hits of each cluster (without weights). This defines the axis of each cluster.
2. The clusters are sorted by their most downstream layers (most downstream hit in the cluster)  $l_{inner}$ .
3. Starting from the most downstream cluster  $i$ , we look for a parent cluster  $j$  for which it propagates further downstream ( $l_{inner,i} > l_{inner,j}$ )
4. Among these candidate parent clusters, we look for those for which  $d_{proj} < d_{proj,cut}$  and  $\theta_{i,j} < \theta_{i,j,cut}$  where :

- $d_{proj}$  is the distance between the candidate daughter cluster axis and the candidate parent cluster barycentre (line-to-point distance)
- $\theta_{i,j}$  is the angle between the axis of the two clusters

and we choose the cluster for which  $d_{proj}$  is minimal.

5. Among this same list of candidate parent clusters, we look for those satisfying the condition  $d_{cross} < d_{cross,cut}$  and  $d_{closest} < d_{closest,cut}$  where :

- $d_{cross}$  is the distance at closest approach (d.c.a) between the two cluster axes
- $d_{closest,i,j}$  is the closest distance between an object of the parent cluster and the point of closest approach of the cluster axes (distance at closest approach)

and we choose the cluster for which  $d_{cross}$  is minimal.

6. We choose the best candidate parent cluster among the two previous methods above. Many cases may happen i) no parent cluster is found, then no parent cluster is assigned to this daughter cluster, ii) one of the two methods has found a parent cluster or the two methods provide the same parent, then we assign it to the daughter cluster, iii) the two methods have found a parent cluster but there are not the same one. In this case the closest candidate parent cluster among the two in terms of barycentre distance is assigned to the daughter cluster.

7. If no parent cluster has been found for a cluster, nothing is done.

8. If the parent cluster has no associated track, merge the two clusters, otherwise we define the variable  $\Psi$  as :

$$\Psi = \left| \frac{p - E_{tot}}{f_{res} \cdot \sigma_E \cdot p} \right| \quad (A.3)$$

where :

- $p$  is the track momentum of the parent cluster
- $E_{tot}$  is the total energy estimated from the combined hit list of the parent and daughter clusters
- $\sigma_E$  is the calorimeter energy resolution at the track momentum  $p$
- $f_{res}$  is a multiplicative factor<sup>4</sup>

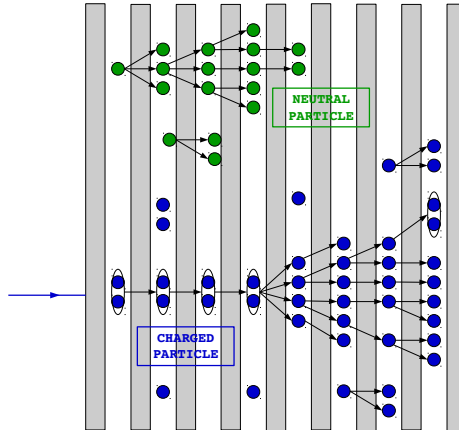


Figure 15: Schematic view of the final ArborPFA output

<sup>4</sup>The parameter  $f_{res}$  is used to reduce or enlarge the accepted range of the difference  $p - E_{tot}$ . A higher value of this parameter will accept a merging with a higher difference  $p - E_{tot}$ .

401 We check then that the  $\Psi$  defined for the parent and daughter clusters is less than  $\Psi_{cut}$  and  
402 if the difference between  $p$  and  $E_{tot}$  after the cluster merging (parent + daughter clusters)  
403 decreases. The two clusters are merged if the previous conditions are satisfied.

404 **Small neutral fragment merging** At this stage, the main part of the shower of each particles has  
405 been identified. Only isolated objects and small tree structures that surround the showers are not  
406 associated. First, these small structures are identified if their size is less than  $N_{cut}$  objects. Then  
407 every small structure is merged within a shower, the closest in terms of barycentre distances.

408 **Particle flow object creation** Particle flow objects are built from the produced clusters after all  
409 the steps described above (Figure 15). Charged PFOs are built from clusters that have an associated  
410 track, while other clusters are considered as neutral PFOs.

411 **B. ArborPFA algorithm parameters**

412 **Object creation algorithm**

Parameter name	value
MaxClusterSize	4
IntraLayerDistance	11 mm

- 413 • MaxClusterSize  
414 → The maximum intra layer cluster size to build an object with. Else the object is split in  
415 single calo hit objects
- 416 • IntraLayerDistance  
417 → The nearest neighbour intra layer clustering maximum distance

418 **Track segment candidate tagging algorithm**

Parameter name	value
MaxNNeighbors	6
IntraLayerNeighbourDistance ( $\Delta_{mip}$ )	50 mm

- 419 • MaxNNeighbors  
420 → The maximum number of neighbouring objects within a layer
- 421 • IntraLayerNeighbourDistance ( $\Delta_{mip}$ )  
422 → The maximum distance between two neighbours in a layer used for the neighbour count-  
423 ing

424 **Primary track connection**

Parameter name	value
ConnectionDistance	110 mm
BackwardConnectorWeight	2
ForwardConnectorWeight	3
OrderParameterAnglePower	1
OrderParameterDistancePower	5
MaxNEmptyConsecutiveLayers	3

- 425 • ConnectionDistance
- 426 → The maximum connection distance used for the primary track connectors creation
- 427 • BackwardConnectorWeight ( $w_{bck}$ )
- 428 → The backward connector weight assigned for the reference vector computation
- 429 • ForwardConnectorWeight ( $w_{fwd}$ )
- 430 → The forward connector weight assigned for the reference vector computation
- 431 • OrderParameterAnglePower
- 432 → The angle power parameter of the  $\kappa$  parameter while cleaning connectors
- 433 • OrderParameterDistancePower
- 434 → The distance power parameter of the  $\kappa$  parameter while cleaning connectors
- 435 • MaxNEmptyConsecutiveLayers
- 436 → The maximum consecutive empty layers to take into account for the connector seeding

437 **Connector seeding 1**

Parameter name	value
ConnectionDistance	45 mm

- 438 • ConnectionDistance
- 439 → The maximum connection distance used for a connector creation



## 440 Connector cleaning 1

Parameter name	value
BackwardConnectorWeight	2
ForwardConnectorWeight	2
OrderParameterAnglePower	1
OrderParameterDistancePower	5
ReferenceDirectionDepth	1

- 441 • BackwardConnectorWeight
- 442 → The weight of a backward connector assigned in the reference direction vector calculation.
- 443 • ForwardConnectorWeight
- 444 → The weight of a forward connector assigned in the reference direction vector calculation.
- 445 • OrderParameterAnglePower
- 446 → The  $\theta$  angle power parameter used for the  $\kappa$  parameter computation
- 447 • OrderParameterDistancePower
- 448 → The  $\Delta$  distance power parameter used for the  $\kappa$  parameter computation
- 449 • ReferenceDirectionDepth
- 450 → The forward connector depth used for the reference vector computation

## 451 Connector seeding 2

Parameter name	value
ConnectionDistance	65 mm
ConnectionAngle	0.7 rad

- 452 • ConnectionDistance
- 453 → The maximum connection distance used for a connector creation
- 454 • ConnectionAngle
- 455 → The maximum angle between two connectors

## 456 Connector cleaning 2

Parameter name	value
BackwardConnectorWeight	0.1
ForwardConnectorWeight	5
OrderParameterAnglePower	1
OrderParameterDistancePower	5
ReferenceDirectionDepth	2

- 457 • BackwardConnectorWeight  
458 → The weight of a backward connector assigned in the reference direction vector calculation.
- 459 • ForwardConnectorWeight  
460 → The weight of a forward connector assigned in the reference direction vector calculation.
- 461 • OrderParameterAnglePower  
462 → The  $\theta$  angle power parameter used for the  $\kappa$  parameter computation
- 463 • OrderParameterDistancePower  
464 → The  $\Delta$  distance power parameter used for the  $\kappa$  parameter computation
- 465 • ReferenceDirectionDepth  
466 → The forward connector depth used for the reference vector computation

## 467 Energy driven track cluster association

Parameter name	value
TrackToClusterDistanceCut1	75 mm
TrackToClusterDistanceCut2	55 mm
FirstInteractingLayerNSeedCut	15
TrackToClusterNLayersCut	3
TrackClusterPsi2Cut	3
Psi2SigmaFactor	1.5

- 468 • TrackToClusterDistanceCut1  
469 → The maximum distance between the track projection at calorimeter front face and a cluster  
470 seed. This distance is used to detect an early interacting cluster.
- 471 • TrackToClusterDistanceCut2  
472 → The reduced maximum distance between the track projection at calorimeter front face and  
473 a cluster seed. This distance is used when no early interacting cluster has been detected.

- 474 • FirstInteractingLayerNSeedCut  
475 → The cut on the number of cluster seeds found within a the distance TrackToClusterDis-  
476 tanceCut1 to detect an early cluster interaction.
- 477 • TrackToClusterNLayersCut  
478 → The number of inner layers to look for cluster seeds to associate.
- 479 • TrackClusterPsi2Cut  
480 → The  $\psi^2$  cut applied while associating clusters to a track.
- 481 • Psi2SigmaFactor  
482 → The  $f_{res}$  factor on denominator used to compute the  $\psi^2$  for track-to-cluster compatibility  
483 (see equation A.3)

#### 484 Neutral tree merging

Parameter name	value
SeedSeparationMerge ( $\Delta_{seed}$ )	25 mm

- 485 • SeedSeparationMerge ( $\Delta_{seed}$ )  
486 → The maximum distance between two cluster seeds within a layer to perform a cluster  
487 merging

#### 488 Pointing cluster association

Parameter name	value
MinNObjects	4
MinNLayers	4
FitToBarycentreDistanceCut	30 mm
FitToBarycentreAngleCut	$\frac{\pi}{6}$ rad
FitToFitDistanceCut	20 mm
FitDistanceApproachCut	20 mm
Chi2NSigmaFactor	1.5
Chi2AssociationCut	1

- 489 • MinNObjects  
490 → The minimum number of objects within a cluster in order to to be candidate for the  
491 pointing cluster association
- 492 • MinNLayers  
493 → The minimum number of layers within a cluster (outermost - innermost + 1) in order to  
494 be candidate for the pointing cluster association

- 495 • FitToBarycentreDistanceCut  
496 → The cut applied on the distance between the daughter cluster fit and the parent cluster  
497 barycentre position (point-to-line distance)
- 498 • FitToBarycentreAngleCut  
499 → The cut applied on the angle between the daughter and parent cluster fits
- 500 • FitToFitDistanceCut  
501 → The cut applied on the distance between the daughter and parent cluster fits (line-to-line  
502 distance)
- 503 • FitDistanceApproachCut  
504 → The cut applied on the closest distance between a parent cluster object and the daughter  
505 cluster crossing point at the parent and daughter cluster fit closest approach.
- 506 • Chi2NSigmaFactor  
507 → The  $N_{res}$  factor on denominator used to compute the  $\chi^2$  for track-to-cluster compatibility  
508 (see equation A.3) using the merged cluster (daughter + parent)
- 509 • Chi2AssociationCut  
510 → The  $\chi^2$  cut applied on the merged clusters compatibility with a track when associating a  
511 neutral daughter cluster with a charged parent cluster.

#### 512 **Small neutral fragment merging**

Parameter name	value
MaximumDaughterNObject	20
LargeDistanceCut	1000 mm

- 513 • MaximumDaughterNObject  
514 → The maximum number of objects to consider the cluster as a small neutral fragment to  
515 merge it into a bigger parent cluster
- 516 • LargeDistanceCut  
517 → The maximum distance between a small neutral fragment and a potential parent cluster